

# GE 1.5 XLE Wind Turbine Blade Analysis with Computational Methods for Various Composite Materials

EFSTATHIOS E. THEOTOKOGLOU, GEORGIOS XENAKIS  
Department of Mechanics, Laboratory of Testing and Materials,  
School of Applied Mathematical and Physical Sciences,  
National Technical University of Athens,  
Zografou Campus 15773, Athens,  
GREECE

*Abstract:* - The purpose of this paper is to investigate various composite materials that have been applied in wind turbine blades. A computational study on a GE 1.5 XLE wind turbine blade with different composite materials was performed. The computational evaluations from the fluent analysis have been used in order to calculate the equivalent (Von-Mises) stress, shear stress, and displacements of a wind turbine blade. The proposed study results in useful and interesting conclusions for the stress and displacement fields that arise in blades with different materials and under different loading conditions.

*Key Words:* - Composite materials, Computational analysis, Renewable energy, Wind turbine blades, Fluent analysis, Structural analysis

Received: January 19, 2023. Revised: March 22, 2023. Accepted: April 8, 2023. Published: May 19, 2023.

## 1 Introduction

In the last few years, our planet's environment has been exponentially destroyed, the earth's population is growing, mineral wealth is steadily diminishing, and its management is a matter of concern to humans and states. We consume the earth's energy reserves without thinking about future generations. Turning to renewable energy is essential for our survival. Wind energy (via wind turbines) appears as an ideal solution to the problem, [1], [2], [3], [4], [5], [6], [7], [8], [9].

In order to use the wind turbines, we have to improve the profit from their use. One way to maximize profit is to optimize manufacturing. This can be done either by improving the geometry of the construction or its materials. Many studies have been carried out on both cases. There are relevant studies, [6], [7], on the geometry and the effect of air on wind turbine blades. Another way to optimize the geometry to avoid buckling is presented in [10]. In terms of new materials applied in wind turbine blades more and more research has been done in recent years, [12], [13]. The main component of the wind turbine that can be improved is the blade.

During its operation, the wind turbine blade receives complex loads of varying intensity and orientation. In order to withstand all these loads, manufacturers place great emphasis on the material to be used in their manufacture. Experience has

shown that suitable materials are fibrous polymer composites. A detailed comparison between glass and carbon fiber takes place in [9]. Today, the largest range of wind turbines has E-glass composite material as the wind turbine blade material. However, many studies, [14], [15], [16], [17], [18], [19], [20], [21], [22], [23], [24], [25], [26], [27], [28], [29], [30], [31], are being carried out to develop new, stronger, more durable, and easily repairable materials.

Many wind turbine installations worldwide have been studied for their failure problems. The main problem seems to be due to fatigue on the flaps. Fatigue blades are either repaired or replaced. Experience from the failures of wind turbines over the years has led to a knowledge of the design of composite materials for their manufacture. Manufacturers, with increased knowledge, optimized the design of the blades and increased their life expectancy and reliability, [2].

However, not only the failures but also the increase in the size of the wind turbine blades pushed the designers to change their approach to wind turbine design. In the eighties, designers used only static or almost static analysis. This led to constructions with too much material or failures after a few operating cycles. Programmable dynamic models are now used, which simulate unstable aerodynamic loads as well as aerosol responses of the entire wind turbine. In addition,

inspections, non-destructive controls as well as maintenance programs are involved in the production process so that designers gain thousands of hours of experience in wind turbine operation, [2].

Many studies on fiber development, [32], which are stronger than E-glass fibers, have been carried out. High-strength fibers (which are rarely used in practice but make a promising source for improving composites) are carbon, basalt, and aramid fibers. Glass, carbon, and aramid are the most common fibrous reinforcement contained in polymer matrices. Other fibrous materials are boron, silicon carbide, and aluminum oxide.

In this study, five different materials were analyzed in a single wind turbine blade. These are promising materials according to [1], ideal for wind turbine blades. The materials to examine are E-glass, Kevlar aramid, Solvay APC-2 / AS4 carbon fiber, S-glass, and S-2 glass. They all have a common polyester matrix material and as reinforcing materials glass fibers, carbon fibers, and aramid fibers (Table 1). In addition, all materials are placed in the same geometry, with the same thickness, under the same boundary conditions. The scope of this study is to shed some more light on the behavior of GE 1.5 XLE wind turbine blades under different material combinations and loading conditions in order to improve it.

## 2 Materials used in This Study

Fiberglass is simply a composite of glass fibers, continuous or discontinuous, contained in a polymeric matrix. This type of composite material is produced in very large quantities. The diameters of the fibers usually range from 3 to 20  $\mu\text{m}$ . Glass is very popular as a fibrous reinforcing material for many reasons, [3]:

- It is easily pulled from the melt on high strength fibers.
- It is readily available and can be produced in glass-reinforced plastic using a wide variety of composite manufacturing techniques.
- As a fiber, it is relatively strong and when immersed in a plastic die produces a composite material that has very high specific strength.
- When coupled to various plastics it has a chemical inertness, which makes the composite useful in a wide variety of corrosive media, [3].

Carbon fibers with the chemical name “poly-metaphenylene isophthalamides” are high performance fibers and they are the most widely used reinforcing agents in advanced (non-

fiberglass) polymeric matrix composites, [3]. Their features are:

- Of all fibrous reinforcing materials, carbon fibers have the highest specific modulus of elasticity and the highest specific strength.
- They maintain high tensile strength and high resistance to high temperatures. However, oxidation at high temperatures can be a problem.
- At room temperatures, carbon fibers are not affected by moisture or a wide variety of solvents, acids, and bases.
- Their fibers exhibit a range of physical and mechanical properties enabling the composites containing them to have specially designed properties.
- Fiber production processes have been developed for composites that are relatively inexpensive and cost effective, [3].

Furthermore, aramid fibers are high strength and high elasticity materials that were produced in the early 1970s. They are advantageous for their excellent values of strength ratios by weight and are superior to those of metals. There are many types of aramid materials. The trade names of the two most common types are Kevlar and Nomex. The former is classified according to its mechanical properties in Kevlar 29, Kevlar 49, and Kevlar 149, [3]. In this study, Kevlar 49 is used.

## 3 Overview of Blade Damage

Exact information on the range of wind turbine failures is not generally available; however, studies of composites and damage to contact points have been conducted in recent years, [6], [7]. The static loads and the load cycles applied to the blades are simulated in tests and vary in different layers, fiber layers or surfaces, compression failures, and cracks at various points. Obviously, the failures in the main beams and the root and acoustic layers are the most critical. Fortunately, the composites are durable. However, the onset of failures does not occur on external surfaces and is not easily visible. In addition, many cracks result from the concentration of stresses at the ends of the length of one layer. Still, other cracks can be found visually but the depth of the cracking is not easily detectable, [1].

In addition to the loads to which wind turbines are subjected, they can be subjected to lightning, natural disasters, or intense humidity. In some rare cases, a bolt of lightning can cause destruction. Wind turbine maintainers try to predict the weather as much as possible, but at 25 years of operation, it

is assumed that the wind turbine suffers some disasters, [1].

Wind turbine blades are the most likely to be exposed to lightning and usually receive a significant number of blows during operation. Of course, all parts of the wind turbine have a lightning protection system. However, it is common for burned surfaces or cracks to occur around the point of a lightning strike, [1].

Another significant number of failures was observed in the blades due to the rough gaseous particles that hit and corrode the outer surfaces, especially at the edge where the speeds are higher. As the surface changes, the aerodynamic efficiency of the blades was degraded and energy production is reduced. The more the failure repaired, the greater the damage, more time, and more methods that are complicated are required to repair it, [1].

There is also the case of failure due to ice. At low temperatures, ice forms on the surface of the blades, which disturbs the balance of the aerodynamic loads and reduce the structural fatigue resistance, [1].

Structural failure in a wind turbine can occur in any structural component; however, the most common type of failure is in the rotor or the blade. The cost of a blade corresponds to 15-20% of the total cost of the wind turbine, and repairing is the most expensive work that can be done. According to them, the structural life of the blades is considered important. In addition, the imbalance in rotational forces due to blade failure can lead to significant damage to the entire wind turbine system, and to the collapse of the entire tower if no corrective action is taken, [1].

A number of ways have been invented to detect failures, as well as to measure displacements, either by metering sensors or by acoustic emissions. The types of wind turbine failures are:

- Shape damage and failure development between cover welding and main beam flange.
- Shape damage and failure development between the top and bottom flap weld peripherals of the shell.
- Shape destruction and failure development between body and face interface in sandwich composites both externally and in main beams.
- Inner shape destruction and failure development in laminates peripherally or in the main beam under tensile or compressive loads.
- Rapid propagation of fiber cracks in the periphery or main beam.
- Bending in the periphery due to shape failure or development failure in the connection between main beams and peripheral under compressive

loads.

- Development of cracks in layers and separation of layers from coating, [2].



Fig. 1: Levels of wind turbine blade inspections

When designing and manufacturing wind turbine blades various tests are performed to assess the quality of the materials. As shown in Figure 1, the main pyramid-shaped levels have been created. To have the blades of an IEC 61400 wind turbine certified, [1], they must have passed the first and third level control, [1].

In the first level of controls, small samples of the blade materials are subjected to tests to determine their properties and their fatigue resistance. These checks are usually inexpensive and easy to execute.

In the second level of controls, larger pieces are subjected to more complex controls. The purpose is to verify computational models for critical details. It is generally a more expensive procedure, which is why it is performed less frequently.

In the third level of controls, the blades are examined both dynamically and statically based on the requirements of IEC 61400-23, [1]. Full-scale tests are typically performed on one or two blades to confirm that they meet the design specifications. The total cost of controls at this level is very high as it can take several months to complete. Also important is the cost of waiting for the product to hit the market.

In the finite element simulation work presented by [8], it is proved that the controls at the edge of the blades in traction forces give satisfactory results. Failure loads as well as material failures are identical to third-level controls.

At the moment, standard IEC 61400-23 and DNVGL-ST-0376 quality tests are performed in two directions, flap wise and edgewise, one direction at a time.

During operation, the blades of wind turbines are subjected to high dynamic loads, resulting in many charge cycles in different directions, centrifugal loads, various turbulences, shear

stresses, and sudden changes in air direction. All of the above lead to significant failures due to fatigue in the life of the blade. The current simulations for fatigue tests do not adequately represent the forces and actual loads they will receive. Efforts were made to find better controls. One method is to test simulations for fatigue on two axes both flap wise and edgewise. According to the study [11], the above test is more representative and promises a better test for the future of simulation for wind turbine blade stresses, [1].

## 4 Analysis of GE 1.5XLE Wind Turbine Blades

The aerodynamic optimal model of a wind turbine blade corresponds to the lowest possible thickness of the blade design. However, safety is a key prerequisite for its design, which takes into account unknown aspects of its loads, material degradation, and possible flap failure. However, in many cases, the safety factors are excessive and lead to superstructures. In order to more precisely identify safety factors, detailed information on the effects of different loading conditions (high winds, humidity, temperature changes) and parameters on the structures of the composite materials of the blades regarding their durability and life expectancy, are used, [1].

The necessary information can be obtained from computational models or theoretical studies of the behavior of blades under different loading conditions. For the failures, a number of analytical and numerical methods are required. Among the analytical methods used are models based on residual shear stresses, generalized fiber bundle models, failure mechanisms, and mechanism-based models. In the models of residual shear stresses, the equilibrium of forces assumes that shear and fiber loads are transferred only with shear stresses. In general, for fiber bundle models, statistical fiber strength models and different loading conditions are applied. According to previous analyses, the aim is to simulate the failure of composite wind turbines, [1].

Most often problems are solved using the finite element method, in which the integrals and differential equations are calculated describing the material deformations and their microstructure based on the discretization of the bodies and the approximation of the equations. Complex models of wind turbine blades, even with degraded materials, are in the direction of significant analysis through the above methods, [1].

In this study, we analyze the GE 1.5XLE wind turbine blades through the finite element method using at first the ANSYS Fluent program, [5]. The method adopted is the Computational Fluid Dynamics (CFD). The solution arose from the ANSYS 19.2 Workbench software package. Taking into consideration Computer Aided Engineering (CAE) design, simulation, analysis, and processing results, Fluid Fluent and Static Structural, [5], have been used.

The model was manufactured and solved in two parts. First, the Fluent was solved, and then the Structural. The first model was developed to solve aerodynamic loads on the flap and the second through the calculated loads to determine the stresses on the flap and its displacements. The second model was analyzed for five materials. These are E-Glass Fiber, Generic, Solvay APC-2 / AS4 PEEK Plus Carbon Fiber Reinforced Unidirectional Tape, DuPont™ Kevlar® 49 Aramid Fiber, S-Glass Fiber, Generic and S-2 Glass Fiber, Generic. We consider all five materials to be macroscopical isotropic, as they have the same stress values for random directions. The properties of the materials are presented in Table 1, [4]. The work was inspired by a first study by Sebastian Lachance-Barrett, and Robert Zhang Professor of wind energy at Cornell University in New York, [4]. The GE 1.5XLE wind turbine model was manufactured by General Electric. It produces 1500 kW and it operates in minimum winds of 3.5 m/s and a maximum of 20 m/s. It has a wind resistance of up to 52.5 m/s. Its rotor has a diameter of 82.5 meters and covers a surface of 5346 m<sup>2</sup>. It has three blades with a maximum blade speed of 18.7 U/min. It consists of composite material with glass fibers.

### 4.1 Fluent Analysis

The main equations that are used are continuity equations and Navier-Stokes equations. These equations are given below:

- Conservation of mass:

$$\frac{\partial \rho}{\partial t} + \nabla \times \rho \mathbf{u}_r = 0 \quad (1)$$

- Conservation of momentum (Navier-Stokes):

$$\begin{aligned} \nabla * (\rho \mathbf{u}_r * \mathbf{u}_r) + \rho (2\boldsymbol{\omega} \times \mathbf{u}_r + \boldsymbol{\omega} \times \boldsymbol{\omega} \times \mathbf{r}) = \\ = -\nabla p + \nabla * \mathbf{t}_r \end{aligned} \quad (2)$$

Where  $\mathbf{u}_r$  is the relative velocity,  $\boldsymbol{\omega}$  the angular velocity and  $\mathbf{t}_r$  the deviatoric stress tensor. Also,

the Coriolis force appears as  $2\omega \times \mathbf{u}_r$  and the centripetal acceleration as  $\omega \times \omega \times \mathbf{r}$  in the Navier-Stokes equation. In solving Ansys Fluent, [5], we start with the additional terms framed at angular velocity  $\omega = -2\mathbf{k}$ .

Finally, it is used the Reynolds averaged form of continuity and momentum and also the model with the SST k-omega turbulence to complete the set of equations.

We only run 1/3 in hypothetical periodic loads:

$$\mathbf{u}(r_i, \theta) = \mathbf{u}(r_i, \theta - 120n); n = 1, 2, 3 \dots \quad (3)$$

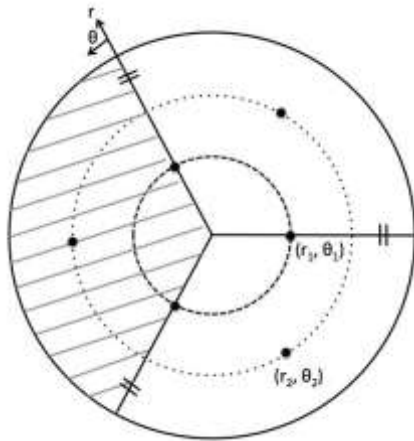


Fig. 2: By taking into account 1/3 of the problem

$$\mathbf{v}(r_1, \theta) = \mathbf{v}(r_1, \theta - 120n); n = 1, 2, 3 \dots \quad (4)$$

$$\mathbf{v}(r_1, 240 - 120(1)) = \mathbf{v}(r_1, 120) \quad (5)$$

$$\mathbf{v}(r_1, 240 - 120(2)) = \mathbf{v}(r_1, 0) \quad (6)$$

$$\mathbf{v}(r_2, \theta) = \mathbf{v}(r_2, \theta_2 - 120n); n = 1, 2, 3 \dots \quad (7)$$

$$\mathbf{v}(r_2, 1800 - 120(1)) = \mathbf{v}(r_2, 0) \quad (8)$$

The above equations prove that the flow velocity distribution at angles 0 and 120 degrees is the same. If  $\theta_1$  represents one of the boundary conditions for 1/3 and  $\theta_2$  the other boundary condition, then  $\mathbf{u}(r_i, \theta_1) = \mathbf{u}(r_i, \theta_2)$ .

Boundary conditions in the fluid region are:

- 1) Inlet (Figure 4): Velocity of 15 m/s with turbulent intensity of 5% and turbulent viscosity ratio of 10.
- 2) Outlet: Pressure 1atm.
- 3) Blade: No slip.
- 4) Side Boundaries: Periodic.

The fluent solver, [5], converts the above differential equations (1) and (2) into a set of

algebraic equations. The conversion of these algebraic equations gives the values  $(\mathbf{u}, \mathbf{v}, p, \omega)$  for each element of the total finite element mesh. Near the flap, we have considered a very fine finite element mesh for better accuracy of the results. The finite element mesh-estimated at about 400,000 triangular and tetrahedral elements (Figure 3). The matrices created are large in volume but considered much sparser as matrices. Ansys, [5], uses a pressure-based solvent. The geometry of the wind turbine was taken from the Cornell University website, [4].

We first observe the fluid (air) in Figure 2, which occupies the bulk volume and encloses one wind turbine blade. The fluid domain is conical in shape with a short radius of 120 m and a long radius of 240 m. Its length is 270 m and the fluid flows from the short beam to the long beam.

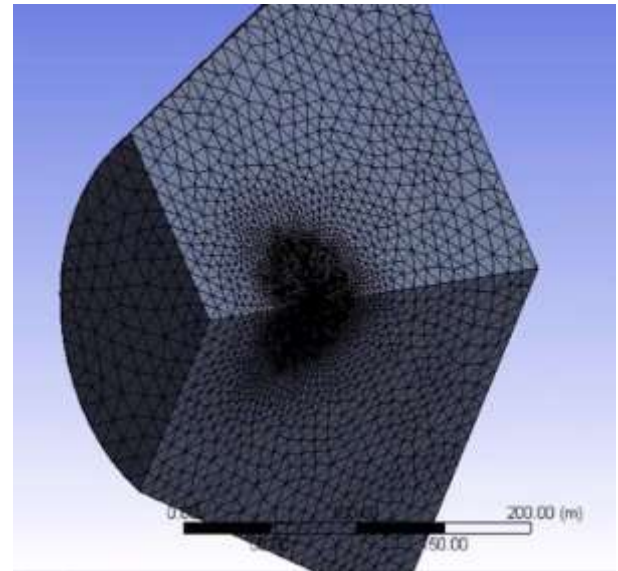


Fig. 3: Total finite element mesh

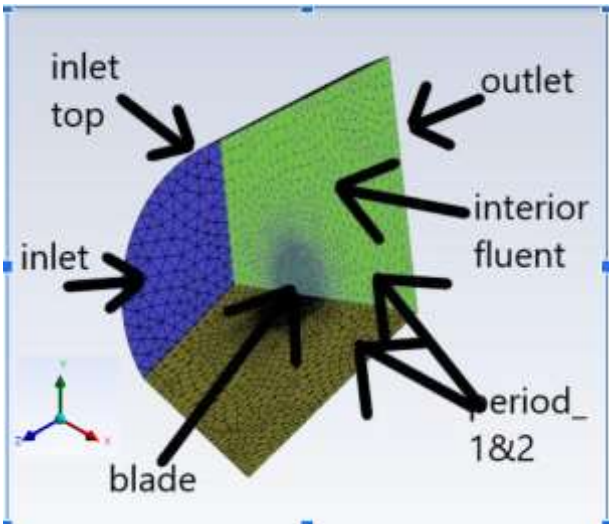


Fig. 4: Various parts that separate the fluid for boundary conditions.

As boundary conditions for speed entry have considered the Inlet sections and the Inlet Top on the Z-axis (Figure 4). A negative speed of 15 m/s on the Z-axis entered. The vortex intensity was 5% and the degree of viscosity was 10. As an outlet, it is obtained a section, which has an outlet pressure equal to atmospheric pressure. In addition, we have considered period\_1 and period\_2 to be interface points, not walls since we have taken 1/3 of geometry. Finally, the type of interior (Figure 4) was included in the fluid section.

With the initial calculations in the pre-analysis, a speed of 88.48 m/s is expected at the ends of the blades and our fluent exported a speed of 88.33 m/s, a result satisfactory for our model (Figure 5).

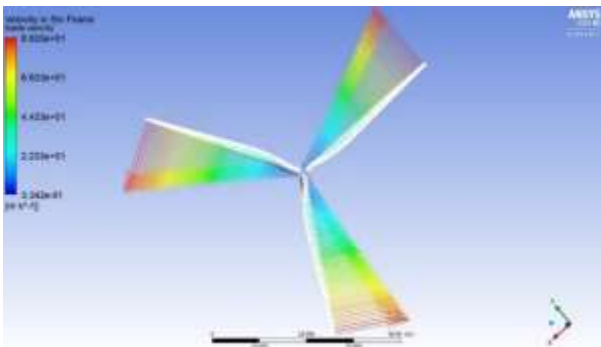


Fig. 5: Air velocity profile with streamline on the blades

Figure 6 shows the wind speed profile from the inlet (inlet) and also from the outlet. Initially, at the entrance, there is a speed of 15m/s, an expected result. Observing behind the blade there is a speed reduction, which indicates correct behavior. Finally, some orange lines around the rotation of

the blades indicate a higher speed, which also indicates a correct solution.

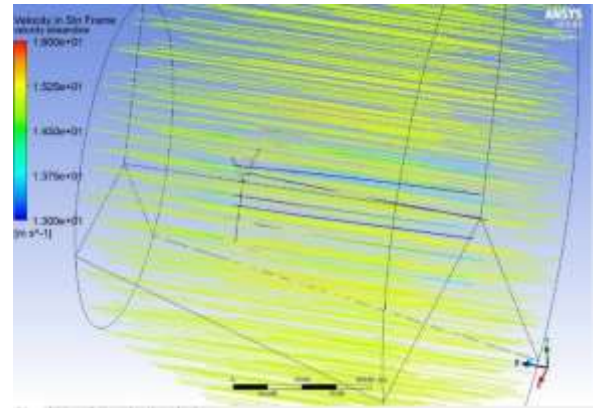


Fig. 6: Air velocity profile

Examine the pressures vertically along the blade on the x-axis (Figure 7). We notice that the maximum pressures are located at the top of the blade which is an expected result.

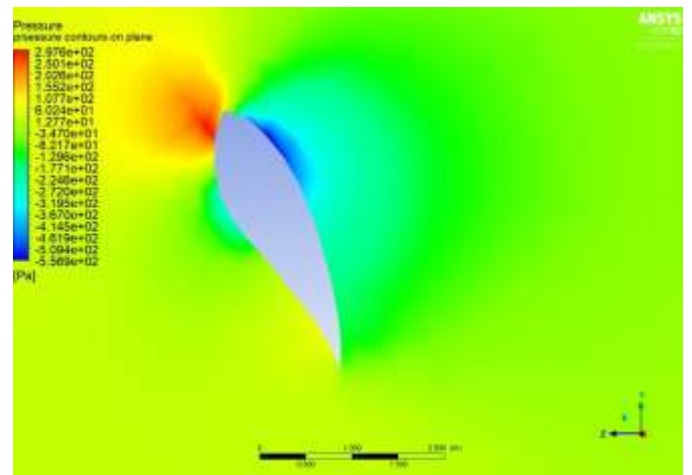


Fig. 7: Pressure around a blade

Then in the next two Figures (Figure 8 and Figure 9) we have a look at the pressure profile on the wind turbine, from the back and the front. As expected, the pressure on the front is greater than on the back.

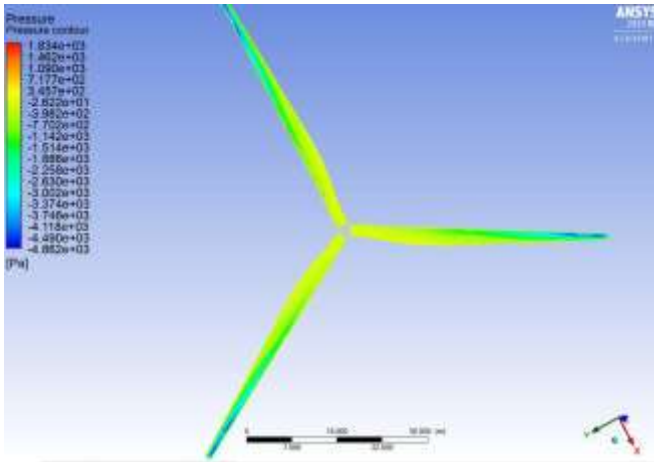


Fig. 8: Pressure profile from the back of the blades

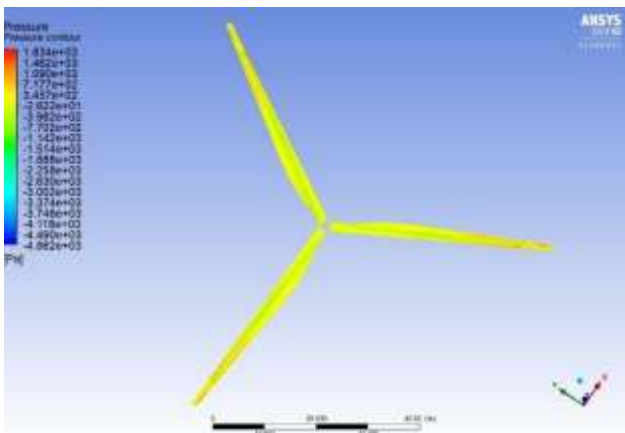


Fig. 9: Pressure profile from the front of the blades

If the shape of the velocity vector is compared with the pressure vector, the results give the expected shape from the buoyancy and the rear of the blade (Figure 10).

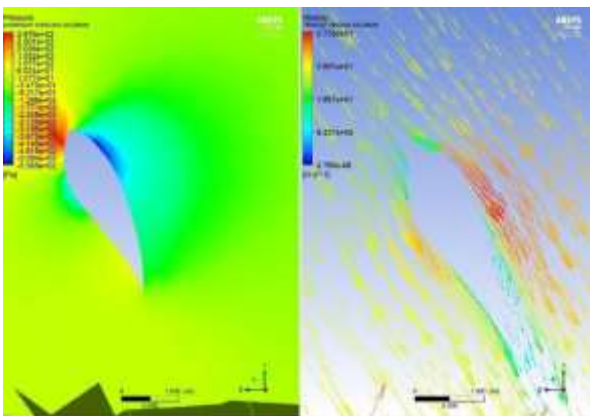


Fig. 10: Speed and pressure around a blade

Another important problem is the solution convergence from the finite element results related to the number of iterations performed. In Figure 11, the behavior of the solution is presented at 3,000 iterations. As we can see, the residuals do not

change much after 1,500 iterations. Therefore, 1,500 iterations are the ideal number to get the right results.

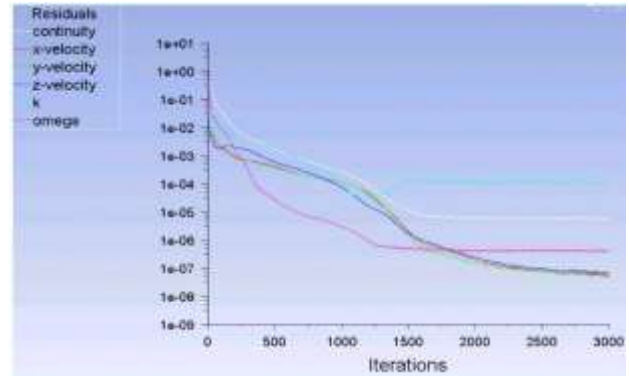


Fig. 11: Solution at 3000 iterations

### 4.2 Structural Analysis

The structural analysis includes the static study of the blade. The pressure on the blade is calculated using the results from the fluent study (section 4.1) and then the stresses and displacements fields are calculated. The blade consists of an outer surface and an inner beam (Figure 12).

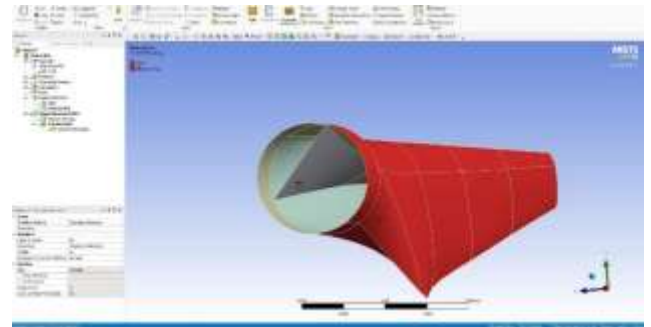


Fig. 12: Separation of the blade into the beam and outer surface

The mathematical model that was used for static analysis is based on Shell theory. This is an extension of Euler-Bernoulli's beam theory, [5].

Table 1. Properties of the materials

Name	Density (Kg/m <sup>3</sup> )	Young Modulus (GPa)	Poisson Ratio	Shear Modulus (GPa)
E-Glass Fiber	2.565	72.4	0.2	30
Kevlar Aramid Fiber	1.437	112	0.36	7
Solvay APC-2/AS4 Carbon Fiber	1.319	138	0.3	5,7
S-Glass Fiber	2.482	86.3	0.22	35
S-2 Glass Fiber	2.457	86.9	0.23	35

In the finite element mesh considered for the blade (Figure 13), an element size of 20 cm was chosen. The program created the best possible mesh with different types of elements (triangular, tetrahedral, etc.). They have been taken about 5,241 finite elements, approximately 90 times less than that in the Fluent analysis.

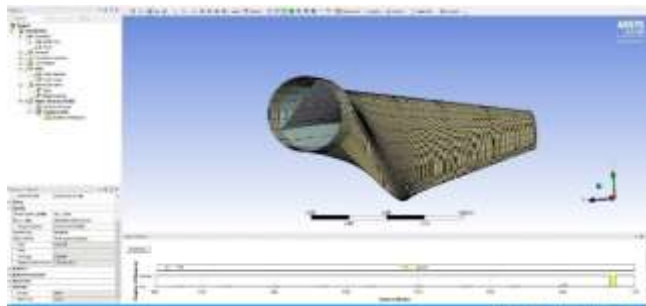


Fig. 13: Blade finite element mesh

At first, the total displacements are calculated. It is observed in Figure 14, that we have the shifts that we expected in the blade. The maximum displacements are created at the tip and when we approach the root of the blade, there is a reduction in displacements in all the examined cases. In Table 2, the maximum displacements according to the different materials are given. It is observed that Solvay APC-2/AS4 Carbon has the maximum displacement.

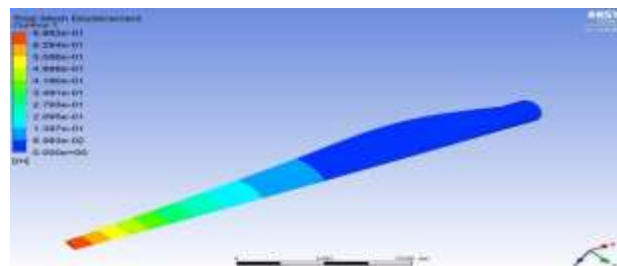


Fig. 14: Overall displacement of E-Glass blade in relation to its original position

Table 2. Maximum displacement

Material	Maximum displacement (m)
E-Glass	0.698
Kevlar/ Aramid	0.488
Solvay APC-2/AS4 Carbon	0.414
S-Glass	0.589
S-2 Glass	0.600

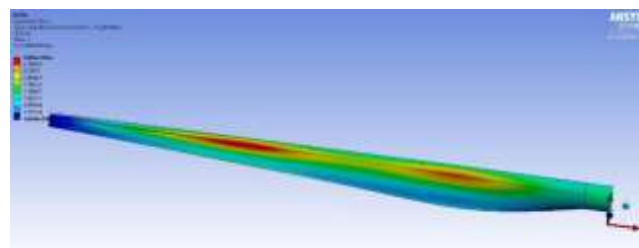


Fig. 15: Stresses profiles on the front of the E-Glass blade

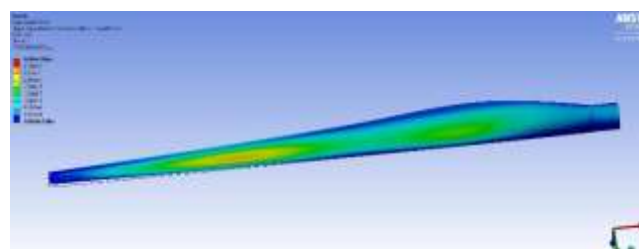


Fig. 16: Stresses profiles in the back of the E-Glass blade

Table 3. Maximum Von-Mises stresses

Material	Maximum Von-Mises stresses (MPa)
E-Glass	30.66
Kevlar 49/ Aramid	32.585
Solvay APC-2/AS4 Carbon	34.084
S-Glass	31.776
S-2 Glass	31.655



In Figure 15 and Figure 16, the Von-Mises stresses are given in the case of the E-glass blade. The area where the maximum stresses occur is the most critical, both in terms of the appearance of cracks and in terms of the manifestation of fatigue. This suggests that the specific blade geometry needs material reinforcement at those points. In addition, the use of stronger material may be a solution to a better confronting of the maximum stresses.

In Table 3 the max Von-Mises stresses according to the different materials are given. It is observed that at Solvay APC-2/AS4 appeared the maximum Von-Mises stress.

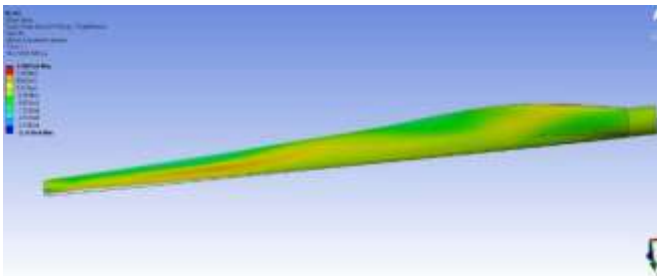


Fig. 17: Shear stresses profile on the back side of the E-Glass blade

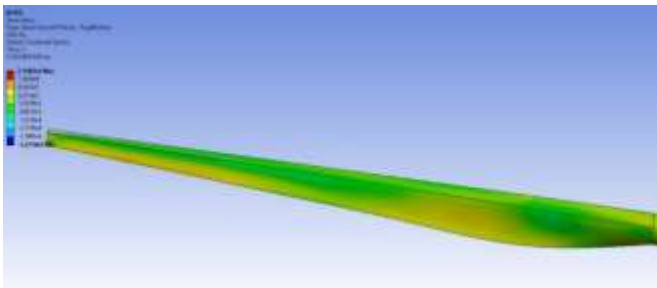


Fig. 18: Shear stresses profile on the front side of the E-Glass blade

Regarding the shear stresses (Figure 17 and Figure 18), we conclude that the maximum shear stresses appear in the same order as that of Von-Mises stresses. The display of the stress profile on the blade is identical to the Von-Mises stresses; the maximum stresses appear at the same points. The values of the maximum shear stresses are summarized in the following Table 4.

Table 4. Maximum Shear stresses

Material	Maximum shear stress (MPa)
E-Glass	2.161
Kevlar 49 /Aramid	1.609
Solvay APC-2/AS4 Carbon	1.251
S-Glass	2.083
S-2 Glass	2.093

## 5 Analysis and Results in Extreme Wind Conditions 60 m/s

Concerning our initial study for 15m/s wind, we conclude that the wind speed profile does not change much. The maximum values at the tip of the blade are around 88m/s, slightly higher. On the contrary, to the previous 15 m/s, the pressure profile has changed significantly. Not so much in terms of the distribution of pressures (Figure 20 and Figure 21) but in terms of their size. More specifically, the maximum pressures are 5,972 Pa; significantly, higher than the 1,834 Pa (Figure 8) we had for wind speed at 15 m/s. The total displacements for wind speed 60m/s have changed significantly too (Figure 19), from 0.6983 m (Table 2) to 1.567 m (Table 5). Furthermore, the maximum Von Mises stresses (Table 6) and the maximum shear stresses (Table 7) have changed significantly.

Lastly, the shear stresses profiles on the back of the E-Glass blade for wind speed 60 m/s are presented in Figure 22.

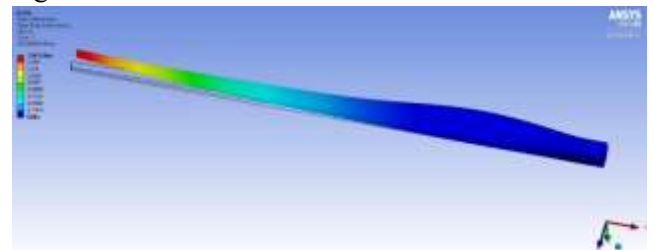


Fig. 19: Overall displacement of E-Glass blade for wind speed 60 m/s

Table 5. Maximum displacements for wind speed 60 m/s

Material	Maximum displacement (m)
E-Glass	1.567
Kevlar 49	1.115
Solvay APC-2/AS4 Carbon	0.945
S-Glass	1.322
S-2 Glass	1.348

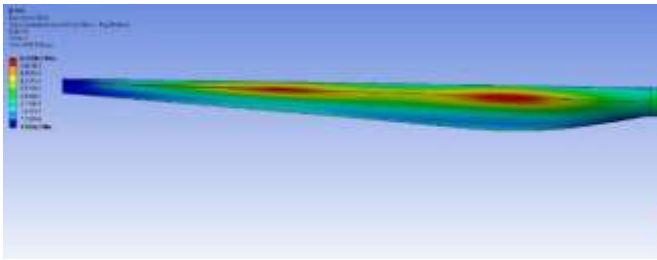


Fig. 20: Stresses profiles on the front of the E-Glass blade for wind speed 60 m/s

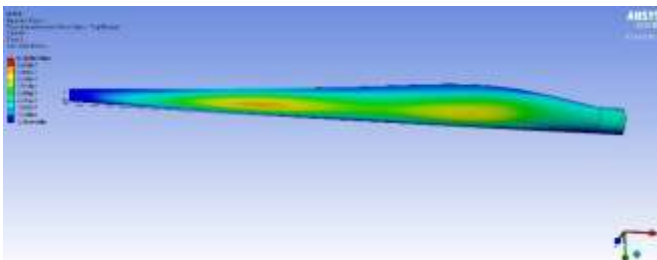


Fig. 21: Stresses profiles on the back of the E-Glass blade for wind speed 60 m/s

Table 6. Maximum Von-Mises stresses for wind speed 60 m/s

Name	Maximum stresses Von-Mises (MPa)
E-Glass	63.22
Kevlar 49	65.47
Solvay APC-2/AS4	69.26
S-Glass	64.45
S-2 Glass	64.24

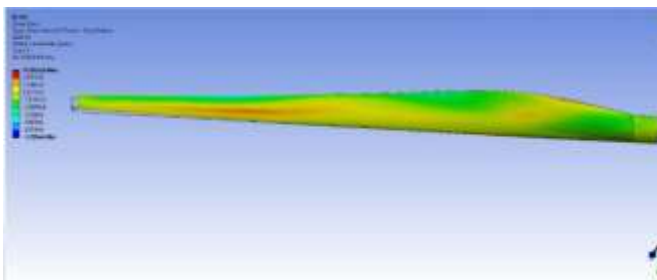


Fig. 22: Shear stresses profiles on the back of the E-Glass blade for wind speed 60 m/s

Table 7. Maximum Shear stresses for wind speed 60 m/s

Material	Maximum shear stresses (MPa)
E-Glass	4.5
Kevlar 49	3.82
Solvay APC-2/AS4	2.89
S-Glass	4.38
S-2 Glass	4.42

## 6 Conclusions

The present work concerned the analysis of a wind turbine blade specifically the GE 1.5 XLE model, through computational methods with various composite materials that are the materials of the future for wind turbines. The materials considered are E-Glass, S-2 Glass, S-Glass, Kevlar 42, and finally Solvay APC-2 / AS4 Carbon. For the study of the proposed materials, a computational analysis is carried out.

Initially, to simulate the model, the pressure which will be exerted on the blade should be calculated. To calculate the pressures, a fluent analysis was performed with a wind simulation of 15m/s. The wind was blowing on the blade from all directions. The form of pressure observed was as expected. The air velocity and the pressure profiles that they extracted were as expected.

Then a static analysis was performed on the blade. The input was the pressure from the fluent analysis. All five materials were analyzed. Von Mises stresses exerted on the materials, shear stresses, and displacements were calculated. The same study for a wind speed of 60 m /s, considered an extreme wind speed, took place, from which much greater pressures have been calculated.

Finally, the results present that the failure rate of the materials used is much lower than the stress limit, so there is no risk of abrupt breakage.

The results also show that the E-Glass material has the highest displacements in both winds. It is followed by the S-2 Glass, the S-Glass, the Kevlar 49, and finally the Solvay APC-2 / AS4 Carbon. This justifies the prices that the materials have in the market, as the most expensive shows the smallest shifts.

It is noted that even in extreme wind conditions (60 m/s) there is no failure of any material. However, the displacements are more than double for each material separately in relation to wind speed under normal conditions (15 m/s), while the stresses are almost double.

In our study for the GE 1.5XLE wind turbine, the stresses and displacements for different blade materials, in normal and in extreme wind conditions, are given. Due to the computer constraints at the nodes and the data of the computational study, the results are considered approximate. Our study may be considered a first step to analyzing a GE 1.5 XLE.

In addition, the proposed study performs one-way-Fluent Solid Interaction (FSI), and the results extracted from the liquid are entered into the solid. An improved version has the ability for two-way-FSI, presenting more accurate results, with a

detailed calculation of the Tangential Force by the coefficients of buoyancy and traction (section 4.1). Ideally, it would be an experimental study to verify the results. The coefficients and variables will be adjusted in such a way that there would be a convergence between a theoretical and an experimental model.

To accurately calculate fatigue, it would be appropriate to use known and tested materials. The simulation of the specimens in fatigue conditions based on the theoretical model would lead to a calculation of the lifespan of the model.

In addition, the stress of corrosion of the materials was not considered. Extreme temperatures or rain conditions can introduce into the model.

Finally, the most important part for future expansion concerns the techno-economic study of the wind turbine. That is, to study the cost of construction for each material in the blade. The difference in performance (due to weight) during its operation and the lifespan of the wind turbine for each of the different materials should be considered. This study will be the criterion for the final selection of the materials that will be used.

#### References:

- [1] Mishnaevsky, L.Jr., Branner, K., Petersen, H.N., Beauson, J., McGugan, M. and Sørensen, B.F., "Materials for Wind Turbine Blades: An Overview", *Materials*, Vol. 10 No. 11, 1285, 2017.
- [2] Sutherland, H.J. and Paul S. Veers, P.S., "Fatigue case study and reliability analyses for wind turbines", *ASME/JSME/JSES Int Solar Energy Conf.*, 1994, pp. 1-7.
- [3] Callister, Jr.W.D., & Rethwisch, D.G., "Materials Science and Engineering an Introduction (EIGHTH EDITION)", John Wiley and Sons, USA., 2018.
- [4] Lachance-Barrett, S., "Investigation of Trailing Edge Sub-Components in Wind Turbine Blades", Master of Science Thesis, Delft University of Technology, 2016.
- [5] ANSYS Engineering Analysis System, *User's manual*, Swanson Analysis System Inc., Houston, USA, 2007.
- [6] Shi, F., Wang, Z., Zhang, J., Gong, Z. and Guo, L., "Influences of wind and rotating speed on the fluid-structure interaction vibration for the offshore wind turbine blade", *Ocean Engineering*, Vol. 84, 2019, pp. 14-19,.
- [7] Zhang, J., Gong, Z., Zhang, X., Guo, L., Hu, D., "Dynamic analysis of offshore wind turbine blades under the action of wind shear and fluctuating wind", *Journal of Vibroengineering*, Vol. 20 No.3, 2018, pp. 1511-1521.
- [8] Branner K., Berring P., Haselbach P.U., "Subcomponent testing of trailing edge panels in wind turbine blades"; *Proceedings of the 17th European Conference on Composite Materials*; Munich, Germany, 26–30 June, 2016.
- [9] Balokas, G. and Theotokoglou, E. E., "Cross-section analysis of wind turbine blades: a comparison of failure between glass and carbon fiber", *Advanced Composite Materials*, Vol. 27, 2018, pp.561-574.
- [10] Theotokoglou, E. E., Balokas, G. and Savvaki, E. K., "Linear and nonlinear buckling analysis for the material design optimization of wind turbine blades", *International Journal of Structural Integrity*, Vol. 10, 2019, pp. 749-765.
- [11] Greaves P.R., Dominy R.G., Ingram G.L., Long H., Court R., "Evaluation of dual-axis fatigue testing of large wind turbine blades", *Proceedings of the Institution of Mechanical Engineers, Part C: Journal of Mechanical Engineering Science*, Vol. 226 No 7, 2011, pp. 1693-1704.
- [12] Ostachowicz W., McGugan M., Schröder-Hinrichs J.-U., Marcin Luczak M., editors, "MARE-WINT .New Materials and Reliability in Offshore Wind Turbine Technology", Springer Open, 2016.
- [13] Mishnaevsky L., Jr., Brøndsted P., Nijssen R.P.L., Lekou D.J., Philippidis T.P., "Materials of large wind turbine blades: Recent results in testing and modelling.", *Wind Energy*, Vol. 15 No 1, 2012, pp. 83-97.
- [14] Brøndsted P., Lilholt H., Lystrup A., "Composite materials for wind power turbine blades", *Annual Review of Materials Research*, Vol. 35, 2005, pp. 505-538.
- [15] Brøndsted P., Nijssen R., editors, "Advances in Wind Turbine Blade Design and Materials", Woodhead Publishing, 2013.
- [16] Walker K., "Renewable Energy Embraces Graphene: Improved Wind Turbine Technology", AZO Cleantech, 2013.
- [17] Watson J.C., Serrano J.C., "Composite Materials for Wind Blades", *Windsystemsmagazine*, Vol. 46, 2010, pp.46-51.

- [18] Mohamed M.H., Wetzel K.K., "3D Woven Carbon/Glass Hybrid Spar Cap for Wind Turbine Rotor Blade", *J. Sol. Energy Eng.*, Vol. 128 No 4, 2006, pp. 562-573.
- [19] Fecko D., "High strength glass reinforcements still being discovered", *Reinforced Plastics*, Vol. 50 No 4, 2006, pp. 40-44.
- [20] Mengal A.N., Karuppanan S., Wahab A.A., "Basalt Carbon Hybrid Composite for Wind Turbine Rotor Blades: A Short Review", *Advanced Materials Research*, Vol. 970, 2014, pp. 67-73.
- [21] Manders P.W., Bader M.G., "The strength of hybrid glass/carbon fibre composites", *J. Mater. Sci.*, Vol. 16, 1981, pp.2233–2245.
- [22] Dai G.M., Mishnaevsky L., Jr. (2014), "Fatigue of hybrid carbon/glass composites: 3D Computational modelling", *Compos. Sci. Technol.*, Vol., 9, 2014, pp. 71-79
- [23] Kalagi G., Patil R., Nayak N. , "Natural Fiber Reinforced Polymer Composite Materials for Wind Turbine Blade Applications", *Int. J. Sci. Dev. Res.*, Vol. 1 No 9, 2016, pp. 28-37.
- [24] Holmes J.W., Sørensen B.F., Brøndsted P. (2007), "Reliability of Wind Turbine Blades: An Overview of Materials Testing"; Proceedings of the Wind Power Shanghai, Shanghai, China, 1–3 November 2007, pp. 1-6.
- [25] Holmes J.W., Brøndsted P., Sørensen B.F., Jiang Z.H., Sun Z.H., Chen X.H., "Development of a Bamboo-Based Composite as a Sustainable Green Material for Wind Turbine Blades", *J. Wind Eng.*, Vol. 33 No 2, 2009, pp. 197-210.
- [26] Sonparote P.W., Lakkad S.C., "Mechanical properties of carbon/glass fibre reinforced hybrids", *Fibre Science and Technology*, Vol. 16 No 4, 1982, pp. 309-312.
- [27] Ma P.C. and Zhang Y., "Perspectives of carbon nanotubes/polymer nanocomposites for wind blade materials", *Renewable and Sustainable Energy Reviews*, Vol. 30, 2014, pp. 651-660.
- [28] Loos M., Yang J., Feke D., Manas-Zloczower I., "Carbon nanotube-reinforced epoxy composites for wind turbine blades", *SPE Plast. Res. Online*, 2012.
- [29] Merugula L.V., Khanna V. and Bakshi B.R., "Comparative life cycle assessment: Reinforcing wind turbine blades with carbon nanofibres", Proceedings of the 2010 IEEE International Symposium on Sustainable Systems and Technology, Washington, DC, USA, 17-19 May 2010, pp. 1-6.
- [30] Loos M.R. and Schulte K., "Is It Worth the Effort to Reinforce Polymers With Carbon Nanotubes? Macromol", *Theory Simul.*, Vol. 20 No.5, 2011, pp. 350-362.
- [31] Thostenson E.T., Li W.Z., Wang D.Z., Ren Z.F. and Chou T.W., "Carbon nanotube/carbon fiber hybrid multiscale composites", *J. Appl. Phys.*, Vol. 91, 2002, 6034.
- [32] Staab G.H., "Laminar Composites". Butterworth-Heinemann; Oxford, UK, 1999:

### Contribution of Individual Authors to the Creation of a Scientific Article (Ghostwriting Policy)

Efstathios E Theotokoglou is responsible for overall supervision, writing the original draft, the writing review, and editing.

Georgios Xenakis is responsible for the Formal analysis, Investigation, Validation, writing of the original draft and the writing review, and editing.

### Sources of Funding for Research Presented in a Scientific Article or Scientific Article Itself

This research was funded by the Empirikion Foundation under the research work "Computational and analytical study of advanced materials for using in wind turbine blades"

### Conflict of Interest

The authors have no conflict of interest to declare.

### Creative Commons Attribution License 4.0 (Attribution 4.0 International, CC BY 4.0)

This article is published under the terms of the Creative Commons Attribution License 4.0

[https://creativecommons.org/licenses/by/4.0/deed.en\\_US](https://creativecommons.org/licenses/by/4.0/deed.en_US)